

## Automatic Classification of the Severity Level of the Retinal Ischemia

N. S. LABEEB<sup>1</sup>, A. HAMDY<sup>2</sup>, IMAN A. BADR<sup>1</sup>, Z. EL SANABARY<sup>3</sup>, A. M. MOSSA<sup>1</sup>, R. Khattab<sup>4</sup>

1) Department of Mathematics, Faculty of Science, Helwan University, Cairo, EGYPT.

2) Department of Communications, Electronics and Computers, Faculty of Engineering, Helwan University, Cairo, EGYPT.

3) Department of Ophthalmology, Faculty of Medicine, Cairo University, Cairo, EGYPT.

4) Department of Ophthalmology, Consultant and Fellow in Helwan University Student Hospital, Cairo, EGYPT.

[dr\\_nada\\_83@yahoo.com](mailto:dr_nada_83@yahoo.com)

**Abstract:** - When the blood vessels stop supplying any region in the retina of the eye, this region is called capillary non-perfusion (CNP). With increasing and spreading of these regions across the retina, the patient can go blind. These regions appear only in the fundus fluorescein angiograms (FFAs). In this paper, an algorithm to automate the segmentation and classification of these regions is presented. The segmentation algorithm consists of three main steps: pre-processing, vessels extraction and CNP segmentation. After that, the automatic classification is applied to determine the severity level of each image. In the segmented algorithm, the CNPs are extracted by using the region growing algorithm. The algorithm is tested on 88 FFA images and evaluated by using two different ground truth images. The severity level is classified based on the percentage of the CNPs in each image.

**Key-Words:** - Retinal ischemia, Classification, Capillary non-perfusion, Ischemia segmentation, region growing.

### 1 Introduction

The earliest organ that is affected by the diabetes mellitus is the retina of the eye and in this case the diabetes is called diabetic retinopathy (DR). The leakage of small vessels in the retina causes the DR due to Hyperglycemia and it could be a silent disease [1]. The DR is divided into two stages: non-proliferative diabetic retinopathy (NPDR) and proliferative diabetic retinopathy (PDR). NPDR starts with microaneurysms and small retinal hemorrhages, then progresses to multiple retinal hemorrhages, cotton wool spots, venous beading, venous loops and ends with intra-retinal microvascular abnormalities, which starts the PDR stage [2]. The Increase of vessels damage leads to capillary non-perfusion (CNP) or retinal ischemia. The regions of the CNP are the regions where the capillary vascular network stops supplying blood to these regions. When these regions spread across the retina and enters its central region (macula) the patient can go blind [3].

The early detection of the DR makes the treatment more efficient. So, to reduce the workload of ophthalmologists and aid in the early diagnosis of the disease, the automatic screening systems are used [4, 5]. These systems can be used to grade the DR [6, 7] or to detect different symptoms of DR. There are symptoms that appear in the color images such as microaneurysms and hemorrhages that occur

as round small dots or blots [8] and exudates that appear as yellowish color [9, 10]. But there is another symptom that does not occur in the color images such as the retinal ischemia that appears only in the fundus fluorescein angiograms (FFAs). Clinically, the retinal ischemia is diagnosed manually by using the FFAs since it appears as dark areas in these images, as shown in Fig. 1. This diagnosis relies on the self-perception of doctors. Because of this, an automated tool is needed to segment the CNP regions and set an objective measure of the spreading level of the disease.

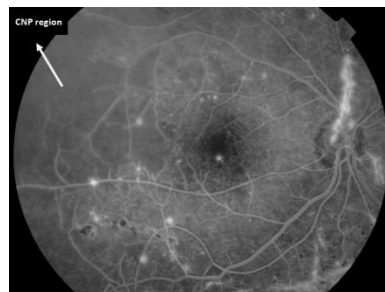


Fig. 1. The CNP region.

There are a few reported methods to segment the CNP regions automatically. The research work in [2] models the CNPs as valleys and performs the valley detection on the FFAs. They do so to locate the seed points in the CNP regions that are used in

the region growing algorithm to extract the candidate CNP regions. Finally, false positive regions are rejected by using a certain threshold. The research work in [11] uses a comprehensive texture segmentation framework to segment the CNPs. In this method, unsupervised texture segmentation is used to segment the candidate CNP regions. Then, these results are refined by a supervised ensemble classifier that is trained with a set of texture features.

In this paper, an algorithm to segment and to classify the retinal ischemia automatically is presented. The algorithm consists of the following steps: pre-processing, extracting vessels, segmenting the CNP regions based on the region growing algorithm and classifying the severity level of the retinal ischemia based on the percentage of the CNPs in the image.

The remainder of this paper is organized as follows: the methodology for the CNP regions segmentation will be discussed in section 2. In section 3, the implementation details and the experimental results are presented. The results are discussed in section 4. Finally, the paper is concluded in section 5.

## 2 CNP Segmentation and Classification Algorithm

In this section, the CNP segmentation method in details will be discussed. This method consists of three main steps: pre-processing, vessels extraction and CNP regions segmentation, as shown in Fig. 2. The ROI is determined and enhanced in the pre-processing stage. Then, the vessels are extracted using the mathematical morphology approach. Finally, the CNP regions are segmented by applying the region growing algorithm. After that, the severity level of the retinal ischemia is classified automatically based on the percentage of the CNPs in the image.

### 2.1. CNP Segmentation

#### 2.1.1. Pre-processing

The basic step in most image processing applications is the pre-processing step. In this step, the image quality can be improved and the region of interest can be determined. At this stage, the background of the image is removed since the normal regions appear as bright white regions and

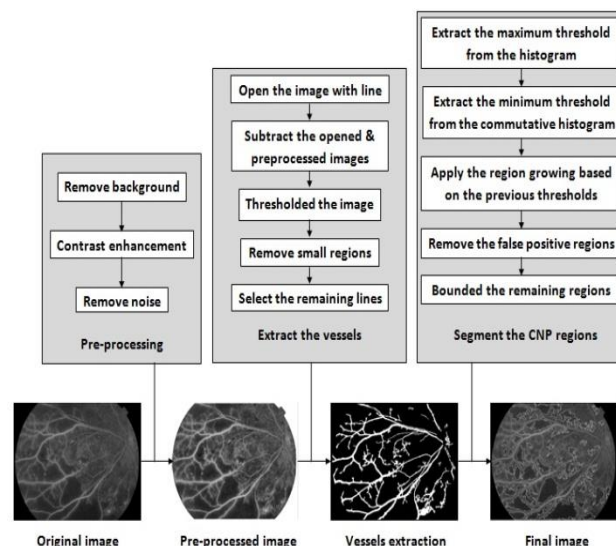


Fig. 2. The flow of the proposed algorithm.

the CNP regions appear as dark regions [2] and the region of interest is determined. Then, the contrast of the image is enhanced. Finally, the noise is removed.

The FFAs consist of a circular region that contains the retina on a semi black background, as shown in Fig. 3. The circular region which is known as the field of view (FOV) will be the region of interest. To remove the black background, a certain threshold was applied on the original image followed by an opening operation with size 50 to remove the smallest regions in the background due to the noise. Then, contrast-limited adaptive histogram equalization [12] with block size  $8 \times 8$ , clip limit 0.01 and number of bins 256 was performed on the FOV. Finally, the median filter with size  $3 \times 3$  was applied to remove the salt and pepper noise with preserving detailed image information [13]. These steps are presented in Fig. 3.

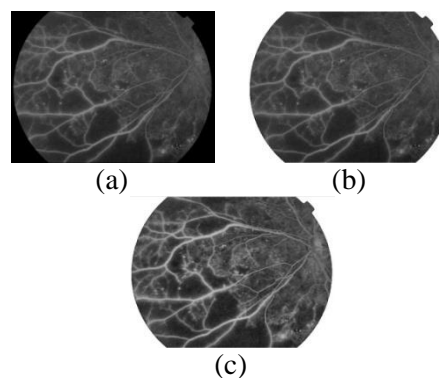


Fig. 3. Pre-processing step, (a) original image, (b) the image after removing background and (c) pre-processed image.

### 2.1.2. Blood Vessels Extraction

The extraction of the blood vessels is an essential step for solving several practical applications such as the registration of patient images obtained at different times, the detection of exudates, the extraction of the optic disc (OD), and the determination of the severity of diabetic retinopathy by calculating the thickness of the blood vessels [14].

There are several algorithms and techniques to extract the vessels. These techniques can be divided into several categories: (1) Multi-scale approaches (2) Skeleton-based (centerline detection) approaches (3) Region growing approaches (4) Ridge-based approaches (5) Differential Geometry-based approaches (6) Matching filters approaches and (7) Mathematical morphology schemes [14], [15].

Since the normal regions and the vessels appear as bright regions in the FFAs, the vessels must be extracted and removed to minimize the brightest regions in the image. To extract the vessels, a method that is based on mathematical morphology like in [16] is applied in our research work because the mathematical morphology technique is the simplest and the fastest technique [14]. First, an opening operation with linear structuring element with twelve rotations (rotate with  $15^\circ$ ) is applied on the original image to remove the linear shape in the image. Then, the resultant image is subtracted from the pre-processed image to emphasize the linear shape in the image. The linear shapes then are extracted by applying Otsu's threshold since it is a robust and speedy threshold [17]. Finally, the smallest noisy regions are removed by applying an opening operation. The results of this stage are shown in Fig. 4.

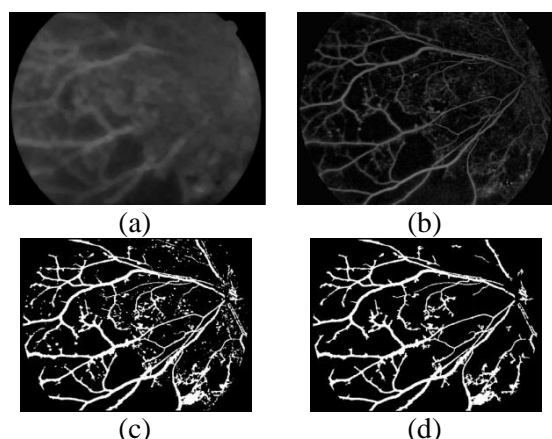


Fig. 4. Extraction of vessels, (a) opened image, (b) difference image, (c) binary image and (d) final image.

### 2.1.3. The CNPs Segmentation

In this final stage, the CNP regions are extracted and bounded by using the region growing algorithm due to its simplicity and good performance [18]. The region growing algorithm groups the pixels or sub regions into larger regions based on predefined criteria. This approach starts with an initial seed point and examines the neighboring pixels to determine if these pixels should be added to this region or not [19].

There are two challenges before segmenting the CNP regions:

1. The CNP region does not have a known size or shape. The only feature that can be used is the CNP's gray level and its texture.
2. Determine the seed point of the region growing automatically.

To solve the first challenge, the CNP regions are manually delineated by expert and these CNPs are then extracted automatically. When the gray level of the extracted CNPs is investigated, one can find that the CNP regions in the same image have the same range of gray levels. This range is smaller than the brightest regions in the image (normal region) and is larger than the darkest region in the image (macula). Also, the CNP region has almost homogeneous texture.

To determine the range of the gray levels of the CNPs in each image automatically, the histogram and the accumulative histogram of the FOV region are used. Firstly, the brightest gray level is determined by taking the maximum of the histogram of the FOV after removing the vessels. This value will be the final value in the range  $T_{max}$ . Secondly, the darkest gray level is determined by using the accumulative histogram of the FOV region. This value will be the first value of the range  $T_{min}$ . The range  $[T_{min} : T_{max}]$  is then used to prevent selecting the darkest regions (such as the macula, blood, hemorrhages) or the brightest regions (such as normal regions) as the CNP regions. This range is also used to reduce the computation complexity time of the region growing algorithm.

Now the seed point of the region growing is selected automatically based on features extraction approaches [18]. So, the algorithm examines each pixel in the FOV region and the pixel that was not on the vessels and its gray level value was in  $[T_{min} : T_{max}]$  range will be the seed point.

After selecting the seed point, the region growing is applied on the FOV region and the candidate CNPs are extracted. Then, the holes in the extracted regions are filled by using set of mathematical morphology such as dilations, complementation and intersections [19]. It should be noted that the CNPs

are not the darkest region in the FOV. Based on this information, the algorithm now examined the extracted candidate regions to ensure that there is no region having gray level smaller than the  $T_{min}$ . If there is a gray level smaller than the  $T_{min}$ , the new value is taken as the new  $T_{min}$  and the region growing is reapplied so the false positive candidates are removed. Finally, the final CNP regions are bounded on the original image. The steps of the CNPs segmentation are presented in Fig. 6. The method to extract the CNP regions can be summarized in Fig. 5:

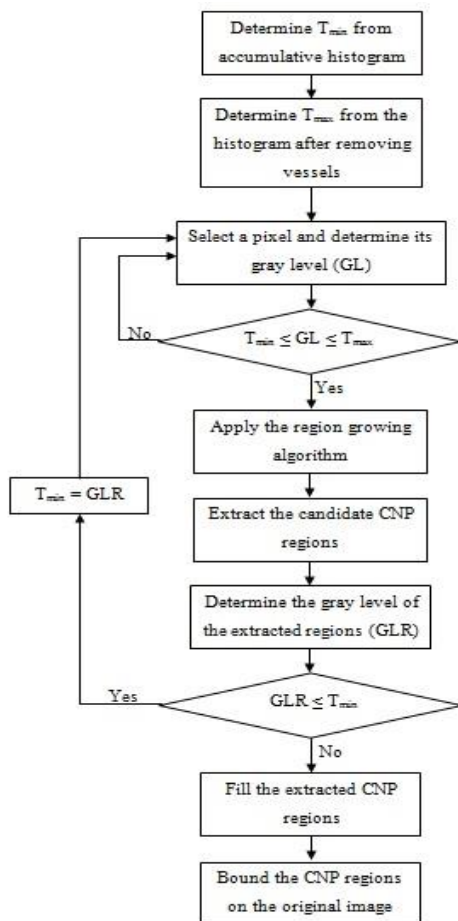


Fig. 5. The CNPs extraction model.

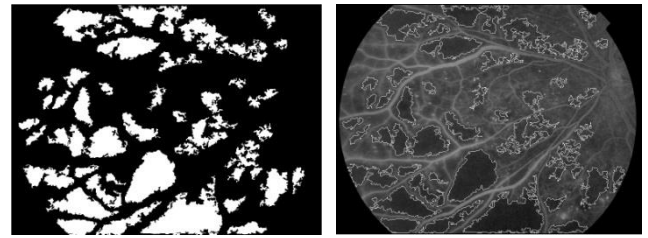
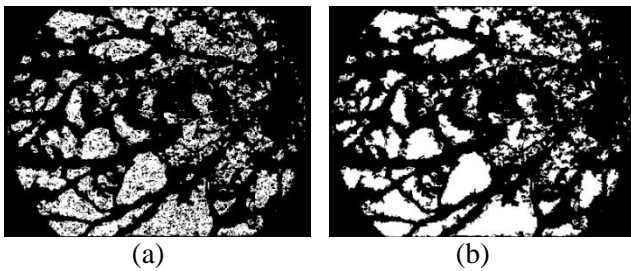


Fig. 6. CNP segmentation, (a) the candidate regions, (b) filled regions, (c) CNP regions and (d) final image.

## 2.2. Classification of the Severity Level of the Retinal Ischemia

In this section, the severity level of the retinal ischemia is classified into mild, moderate and severe based on the amount of the CNPs in the image. The range of each level is determined using Minitab 17 (statistics program). First, the percentages of the CNPs in each image are plotted as seen in Fig. 7.

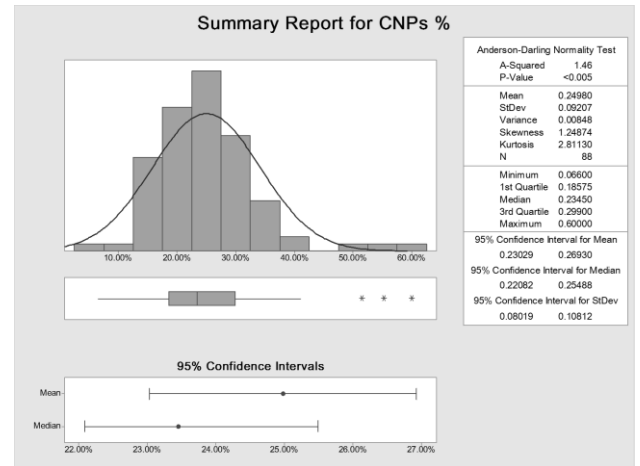


Fig. 7. The CNPs% statistics.

From the box plot in Fig. 7, one can find that the observations of values 51%, 55% and 60% are considered outlier values and should be removed from our data. Then, the new data will be as in Fig. 8.

After that, the test for normality is applied using Kolmogorov - Smirnov with significance level  $\alpha = 0.15$ . Finally, the range of the severity level of the retinal ischemia is calculated based on the mean ( $\mu = 23.90$ ) and the standard deviation ( $\sigma = 7.26$ ) as in Fig. 9. From T-student, the range of the mean is from 23% to 26.93% and from  $\chi$ -square, the range of the variance is from 0.643% to 1.169%. The mild level starts from 0% to 16.64% as in Fig. 11 (a), the moderate level starts from 16.64% to 31.16% as in Fig. 11 (b) and the severe level will be greater than or equal to 31.16%, as in Fig. 11 (c).

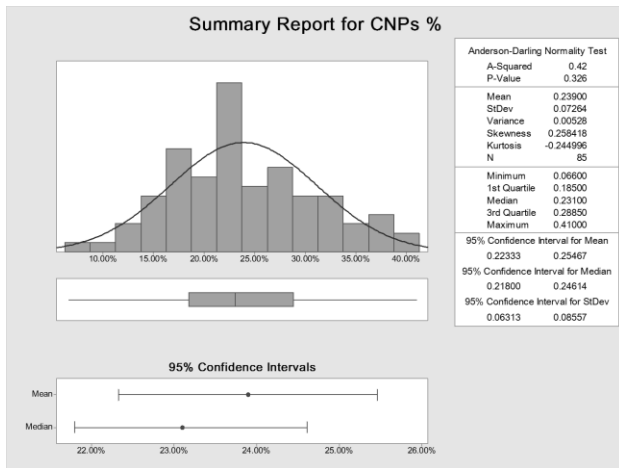


Fig. 8. The new CNPs% statistics.

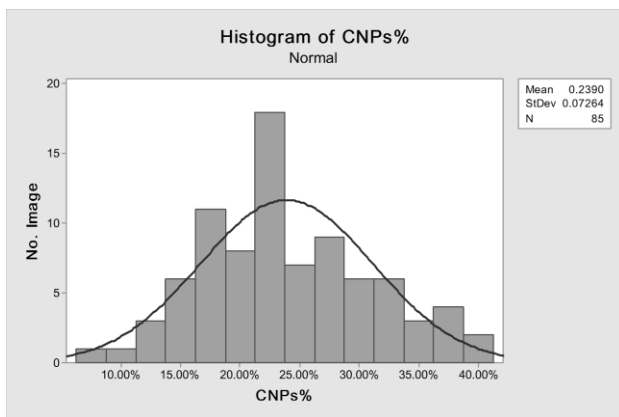


Fig. 9. Normal distribution.

### 3 Implementation and Results

The proposed method is tested on eighty-eight FFA images. These images were taken with 50 degree FOV at a size of 768×576 pixel using a fundus camera (TRC-50 EX, Topcon, Tokyo, Japan). The algorithm is implemented in Matlab 7.0 on a 64-bit operating system (Intel(R) Core (TM) i3 CPU) and all the segmented images were compared and evaluated against two different manual delineations. There are three metrics that are used to evaluate performance: sensitivity, specificity and accuracy. Sensitivity (also called the true positive rate) measures the test's ability to identify the positive pixels (i.e. the CNP pixels in our case). Specificity (also called the true negative rate) measures the test's ability to identify the negative pixels (i.e. the non CNP (normal) pixels in our case). Accuracy measures the performance of the overall classification. These three matrices are defined as follows:

$$Sensitivity (Se) = \frac{N_{CNP}}{N_{TCNP}} \quad (1)$$

Where  $N_{CNP}$  is the number of pixels truly belonging to CNP regions and  $N_{TCNP}$  is the total number of pixels belonging to CNP regions.

$$Specificity (Sp) = \frac{N_n}{N_{Tn}} \quad (2)$$

Where  $N_n$  is the number of pixels truly belonging to normal regions and  $N_{Tn}$  is the total number of pixels belonging to normal regions.

$$Accuracy (Acc) = \frac{N_{TC}}{N_T} \quad (3)$$

Where  $N_{TC} = N_{CNP} + N_n$  is the number of pixels correctly classified and  $N_T = N_{TCNP} + N_{Tn}$  is the total number of pixels.

To create the ground truth images, the experts with different level of experience marked the CNPs in all images manually then these regions are segmented automatically, as in Fig. 10 (b).

After testing the algorithm on the eighty-eight images and comparing with the first delineation, an average sensitivity of 96.4%, specificity of 99.7% and accuracy of 97.7% are obtained. The average running time needed to implement the algorithm was 33.025 seconds and the average ischemic region detection was 97%.

Whereas after comparing with the second delineation, an average sensitivity of 97.9%, specificity of 99.6%, accuracy of 99.3% are obtained and the average ischemic region detection is 96.3%. Fig. 10 presents some of the segmented images compared to the delineated ones. Fig. 11 presents some of examples of the severity level.

### 4 Discussion

The proposed algorithm is tested on 88 images and evaluated against expert-marked ground truth. The contribution of the proposed algorithm is to segment only the CNP regions as complete as possible and eliminate the macula automatically because the reported researches in [11] and [2] segment the macula as a CNP region and eliminate the macula manually. The obtained results achieved average sensitivity, specificity, accuracy and ischemic regions detection greater than the research work in [11].

In [11], a texture segmentation framework is used, and their method is evaluated on 48 images that are taken by using fundus camera and achieved sensitivity of 73%, specificity of 90.8%, accuracy of 89% and ischemic regions detection of 76.3%. But in their work, if the test images contain macula, it was removed manually. While in our research work, the macula is removed automatically.

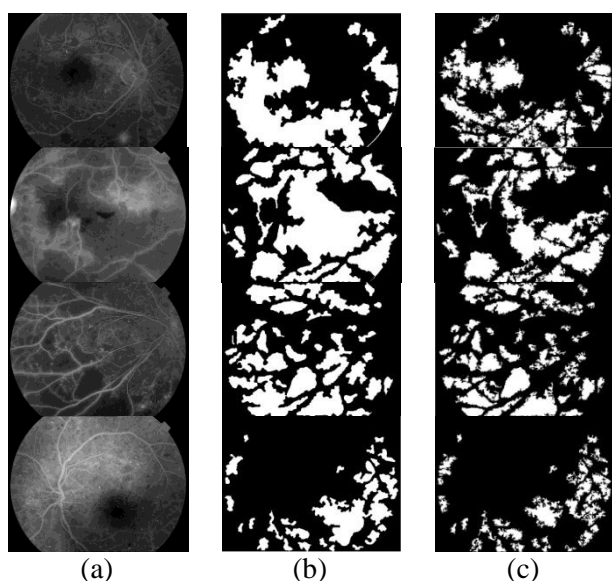


Fig. 10. Segmented images compared with delineated images, (a) original images, (b) delineated regions and (c) segmented regions.

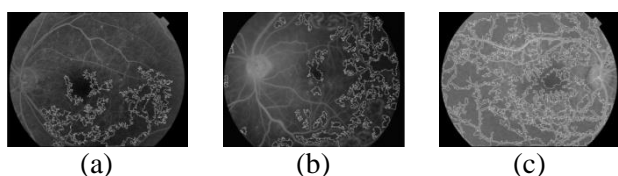


Fig. 11. Examples of the severity level, (a) mild, (b) moderate and (c) severe.

The research work in [2] segmented the CNP regions based on variance-based region growing technique and tested their algorithm on 40 images from the digital confocal scanning laser ophthalmoscope (the quality of these tested images are better than the quality of the tested images in our work) and the obtained results reported an area under curve (AUC) of 0.842 using pixel by pixel evaluation.

## 5 Conclusion

In this paper, an algorithm to extract the CNP regions in the FFAs is presented. This algorithm consists of three steps: pre-processing, vessels extraction, and CNP regions segmentation. In the pre-processing step, the background is removed, the contrast of the image is enhanced, and the noise is removed. The blood vessels are extracted to reduce the brightest areas in the ROI. Finally, the region growing algorithm is used to segment the CNP regions and the severity level is automatically classified based on the percentage of the CNPs in the image.

The automatic segmentation of the CNP regions in FFA images is a difficult task because of different

factors such as the brightness, contrast and artifact. In addition, the position of the CNPs may affect their appearance. For example, the CNPs that appear in the center are different to those at the edge of the FOV and also the regions that are close to the edge of the FOV may appear as CNP due to the poorer focusing problem.

In the future work, the current algorithm can be developed to detect some regions that have similar view to the CNP regions such as hemorrhages [11]. It should be noted that the hemorrhages appear in the color images and FFAs, however the CNPs appear only on the FFAs. So, in the future the hemorrhages are detected from the color images and removed from the FFAs based on image registration between the color and FFA images by using the blood vessels [20] to achieve more accuracy.

## References:

- [1] G. S. Annie and S. Kajamohideen, "Diagnoses of Diabetic Retinopathy by Extracting Blood Vessels and Exudates using Retinal Color Fundus Images", *WSEAS Transactions on Biology and Biomedicine*, Vol.11, 2014, pp. 20-28.
- [2] J. Sivaswamy, A. Agarwal, M. Chawla, A. Rani and Das, "Extraction of Capillary Non-Perfusion from Fundus Fluorescein Angiogram", *Biomedical Engineering Systems and Technologies*, Springer, Berlin, Heidelberg, 2009, pp. 176–188.
- [3] B. R. S. Chandra, "Analysis of Retinal Angiogram Images", *M. S. Thesis*, Dept. Computer Science, International Institute of Information Technology, Hyderabad, India, November, 2005.
- [4] P. C. Siddalingaswamy and K. Gopalakrishna Prabhu, "Automatic Detection of Retinal Features for Screening of Diabetic Retinopathy using Image Processing Techniques", *Phd. Thesis*, Dept. Computer Science and Engineering, Manipal University, Manipal, India, September, 2011.
- [5] O. Faust, U. Rajendra Acharya, E. Y. K. Ng, K. H. Ng and J. S. Suri, "Algorithms for the Automated Detection of Diabetic Retinopathy Using Digital Fundus Images: A Review", *J Med Syst*, Vol.36, 2012, pp. 145–157.
- [6] A. D. Fleming, K. A. Goatman, S. Philip, G. J. Prescott, P. F. Sharp and J. A. Olson, "Automated grading for diabetic retinopathy: a large-scale audit using arbitration by clinical experts", *British Journal of Ophthalmology*, 2010.
- [7] P. C. Siddalingaswamy, K. G. Prabhu and V. Jain, "Automatic Detection and Grading of Severity Level in Exudative Maculopathy",

*Biomedical Engineering: Applications, Basis and Communications*, Vol.23, No.3, 2011, pp. 173–179.

- [8] A. Sopharak, B. Uyyanonvara and S. Barman, “Automatic Microaneurysm Detection from Non-dilated Diabetic Retinopathy Retinal Images Using Mathematical Morphology Methods”, *International Journal of Computer Science (IJCS)*, Vol.38, No.3, August, 2011, pp. 15-24.
- [9] A. Sopharak, B. Uyyanonvara and S. Barman, “Automatic Exudate Detection from Non-dilated Diabetic Retinopathy Retinal Images Using Fuzzy C-means Clustering”, *Sensors*, ISSN 1424-8220, Vol.9, 2009, pp. 2148-2161.
- [10] S. Kavitha and K. Duraiswamy, “Automatic Detection of Hard and Soft Exudates in Fundus Images Using Color Histogram Thresholding”, *European Journal of Scientific Research*, ISSN 1450-216X, Vol.48, No.3, 2011, pp. 493-504.
- [11] Y. Zheng, M. T. Kwong, I. J. C. MacCormick, N. A. V. Beare and S. P. Harding, “A Comprehensive Texture Segmentation Framework for Segmentation of Capillary Non-Perfusion Regions in Fundus Fluorescein Angiograms”, *PLoS ONE*, Vol.9, No.4, 18 April, 2014.
- [12] S. K. Shome and S. R. K. Vadali, “Enhancement of Diabetic Retinopathy Imagery Using Contrast Limited Adaptive Histogram Equalization”, *International Journal of Computer Science and Information Technologies*, Vol.2, No.6, 2011, pp. 2694-2699.
- [13] H. S. Shuka, N. Kumar and R. P. Tripathi, “Median Filter based wavelet transform for multilevel noise”, *Recent Advances in Information Technology (ECCS '14)*, Geneva, Switzerland, December, 2014, pp. 90-95.
- [14] V. Vijayakumari and N. Suriyanarayanan, “Survey on the detection methods of blood vessel in retinal images”, *European Journal of Scientific Research*, ISSN 1450-216X, Vol.68, No.1, 2012, pp. 83-92.
- [15] M. I. Khan, H. Shaikh, A. M. Mansuri and P. Soni, “A review of retinal vessel segmentation techniques and algorithms”, *Int. J. Comp. Tech. Appl.*, ISSN:2229-6093, Vol.2, No.5, September-October, 2011, pp. 1140-1144.
- [16] C. Heneghana, J. Flynn, M. O’Keefe and M. Cahille, “Characterization of changes in blood vessel width and tortuosity in retinopathy of prematurity using image analysis”, *Medical Image Analysis*, Vol.6, 2002, pp. 407–429.
- [17] A. Tigora, “An Image Binarization Algorithm using Watershed-Based Local Thresholding”, *Recent Advances in Image, Audio and Signal Processing (REMOTE '13), (IPPR '13), (ASAP '13)*, Budapest, Hungary, December, 2013, pp. 154-160.
- [18] A. Melouah and R. Amirouche, “Comparative study of automatic seed selection methods for medical image segmentation by region growing technique”, *Recent Advances in Biology, Biomedicine and Bioengineering (HSBS '14)*, Florence, Italy, November, 2014, pp. 91-97.
- [19] C. Gonzalez and E. Woods, “Digital Image Processing”, *3rd Edition*, 2008.
- [20] F. Zana and J. C. Klein, “A Multimodal Registration Algorithm of Eye Fundus Images Using Vessels Detection and Hough Transform”, *IEEE Transactions on Medical Imaging*, Vol.18, No.5, May 1999.